Detailed techno-economic assessment of ammonia as green H_2 carrier

Federica Restelli[a], Elvira Spatolisano[a,], Laura A. Pellegrini[a], Alberto R. de Angelis[b], Simone Cattaneo[b], Ernesto Roccaro[b]*

[a]GASP - Group on Advanced Separation Processes & GAS Processing, Dipartimento di Chimica, Materiali e Ingegneria Chimica "G. Natta", Politecnico di Milano, Piazza Leonardo da Vinci 32, 20133 Milano, Italy

[b]Eni S.p.A. Research and Technological Innovation Department, via F. Maritano 26, 20097 San Donato Milanese, Italy

[*]Corresponding author: Elvira Spatolisano (elvira.spatolisano@polimi.it; phone: +39 02 2399 3207 ; fax: +39 02 2399 3280)

Abstract

Green hydrogen is considered as one of the key measures to tackle climate change. Transport of hydrogen from the most cost-competitive renewable electricity hubs to areas that lack such resources involves the conversion of gaseous hydrogen into a high-density liquid. In the present work, liquefied ammonia is selected as carrier for hydrogen transportation from North Africa to North Italy and the cost of each block of the value chain, synthesis, storage, maritime transport, distribution and cracking, is determined using the levelized cost method. The ammonia synthesis and cracking processes are the cost drivers of the value chain, both in the case of hydrogen utilization in the industrial sector (delivery to a hydrogen valley) and in the mobility sector (delivery to refueling stations). A transport cost in the range of 5.49-6.34 €/kg is obtained for the industrial application and in the range of 6.80-12.22 €/kg for the mobility end use.

Keywords: green hydrogen, ammonia, hydrogen carrier, techno-economic analysis, long distance transport

Abbreviations:

CAPEX	CAPital EXpenditures
CEPCI	Chemical Engineering Plant Cost Index
CW	Cooling Water
DMC	Direct Manufacturing Costs
FMC	Fixed Manufacturing Costs
GE	General Expenses
HRS	Hydrogen Refueling Stations
IEA	International Energy Agency
IFO	Intermediate Fuel Oil
IRENA	International Renewable Energy Agency
LCoHT	Levelized Cost of Hydrogen Transport
LH_2	Liquefied Hydrogen
LNG	Liquefied Natural Gas
LOHCs	Liquid Organic Hydrogen Carriers
LPG	Liquefied Petroleum Gas
OPEX	OPerating EXpenditures

PSA	Pressure Swing Adsorption
RW	Refrigerated Water
WACC	Weighted Average Cost of Capital

Highlights:

- NH_3 assessment as H_2 carrier.
- Ammonia synthesis from green hydrogen.
- Hydrogen destination to H_2 valley and H_2 refueling stations.
- Hydrogen transport costs via maritime transport
- NH_3 value chain: synthesis, storage, transport and cracking.

1. Introduction

Tackling climate change means decarbonizing the global energy system. To achieve this goal, it is necessary to reduce carbon dioxide emissions by substituting fossil fuels with renewable energy sources. Because of the fluctuating nature of the power supplied by renewables, in the next future it will be necessary to adopt secondary energy sources, which can effectively store renewable energy.

Hydrogen (H_2) is one of the secondary energy sources, which produces no greenhouse gas by-products during its utilization, because the oxidation of hydrogen generates only water. Hydrogen can be produced by water electrolysis powered by electricity from renewables.

The most cost-competitive renewable electricity hubs, for example the wind farms of the North Sea or the solar parks of the Middle East, are thousands of kilometers away from the large production sites in Europe. Therefore, storage and supply chain infrastructures need to be developed to move hydrogen through long distances. The main obstacle to gaseous hydrogen delivery is its low volumetric density, which would lead to excessive dimensions of the storage and transport equipment. Several hydrogen carriers have been studied for the purpose of large-scale H_2 delivery. These include ammonia, liquefied hydrogen (LH_2) and liquid organic hydrogen carriers (LOHCs). Ammonia and LOHCs involve the chemical storage of hydrogen by synthesis with nitrogen and organic compounds, respectively. Liquefied hydrogen involves a physical transformation with the aim of increasing the volumetric density. Ammonia is the most promising carrier because the infrastructure for its transport and storage is already developed since it is the second-largest global chemical commodity, utilized as agricultural fertilizer, feedstock for food production, industrial material, refrigerant, and additive. Moreover, unlike LOHCs which are fossil-based compounds, it can be produced by exploiting renewable energy only [1] and, unlike liquefied hydrogen which requires refrigeration to a very low temperature (-253 °C) implying high-quality insulation, it can be stored and transported as a liquid at mild conditions (-33 °C and atmospheric pressure).

State energy departments are funding projects for the development of technologies and processes to implement the use of ammonia as a hydrogen carrier. The American Advanced Research Project Agency-Energy (ARPA-E) granted thirteen projects which aim to improve ammonia production from renewable sources and its conversion back to hydrogen [2]. In the Netherlands, the Gasunie, HES International and Vopak companies have signed a cooperation agreement to develop an import terminal for green ammonia as a hydrogen carrier. The terminal, located at the port of Rotterdam, will be operational from 2026 [3]. In 2020, Air Products, ACWA Power, and NEOM announced a 5 billion $, 4 GW green ammonia plant in Saudi Arabia to be operational by 2025. When commissioned, it will produce up to 1.2 Mt/y of green ammonia [4]. Furthermore, ammonia is considered as hydrogen storage and transport medium in the H21 North of England project [5]. This program, funded by Cadent, Equinor and Northern Gas Networks, aims to convert the North of the UK to hydrogen by 2035. It outlines the potentiality of ammonia for long-term hydrogen supply to the heating market and as an inter-seasonal hydrogen storage method. The International Renewable Energy Agency

(IRENA) and Ammonia Energy Agency (AEA) define ammonia as one of the energy carriers of the 21st century [1].

The value chain of hydrogen delivered in the form of liquefied ammonia (Fig. 1) includes: ammonia synthesis and liquefaction at atmospheric pressure, storage at the loading terminal, maritime transport, storage at the unloading terminal, distribution and cracking. In this value chain, the cost drivers are the synthesis and cracking processes. Therefore, a careful evaluation of their investment and operating costs is needed to perform a reliable economic assessment and to identify cost reduction opportunities.

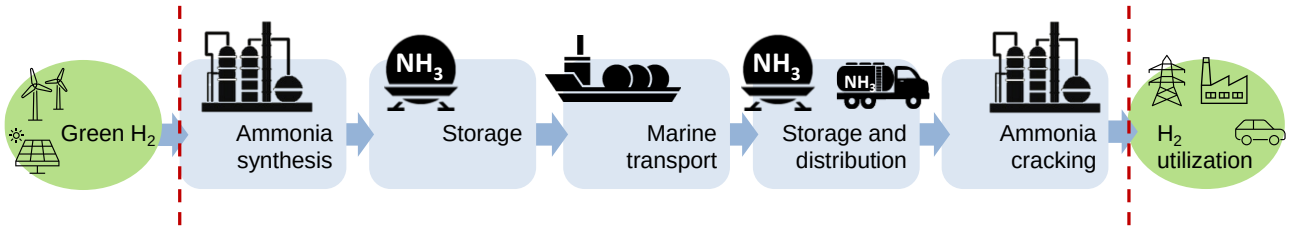

Fig. 1 – Liquefied ammonia as hydrogen carrier.

Techno-economical evaluations on the ammonia value chain are present in literature, especially in comparison with the adoption of other compounds, and are summarized in Table 1.

Table 1 – Techno-economical evaluations on the ammonia value chain available in the literature.

Source	Capacity [t/d]	H_2 source	Export terminal	Import terminal	Other carriers investigated
Okunlola et al., 2022 [6]	607	natural gas reforming + CO_2 capture	Canada (Alberta)	Japan, China, South Korea, Germany, UK	LH_2
Roland Berger, 2021 [7]	20 200	H_2O electrolysis using renewable power (solar power plants)	Middle East (Arabian Gulf)	Europe	LH_2, LOHC (benzyltoluene)
Song et al., 2021 [8]	9000 60000	H_2O electrolysis using renewable power (wind power plant)	China	Japan	LH_2, LOHC (toluene)
Gallardo et al., 2021 [9]	44	H_2O electrolysis using renewable power (solar power plants)	Chile (Antofagasta)	Japan (Osaka)	LH_2
Hong et al., 2021 [10]	1000	natural gas reforming + CO_2 capture and H_2O electrolysis using renewable power	Australia, Malaysia, Indonesia	Singapore	LH_2, LOHC (toluene)
Wood, 2021 [11]	500	natural gas reforming + CO_2 capture	Qatar	United Kingdom	LNG, LH_2, LOHC (toluene)
Papadias et al., 2021 [12]	50	natural gas reforming	Texas, US (Gulf Coast)	North of US	Methanol, LOHC (toluene)
Hydrogen Import Coalition, 2020 [13]	1800	H_2O electrolysis using renewable power	Morocco	Belgium	LH_2, methanol, LNG, LOHC (dibenzyltoluene)

Wijayanta et al., 2019 [14]	900	coal gasification and H_2O electrolysis using renewable power	Australia (Victoria)	Japan (Tokyo)	LH_2, LOHC (toluene)
Hank et al., 2020 [15]	130	H_2O electrolysis using renewable power	Morocco	Germany	LH_2, methanol, LNG, LOHC (dibenzyltoluene)
Ishimoto et al., 2020 [16]	500	90% natural gas reforming + CO_2 capture 10% H_2O electrolysis using renewable power	Norway	Japan (Tokyo) Europe (Rotterdam)	LH_2
IEA, 2019 [17]	700	natural gas reforming + CO_2 capture and H_2O electrolysis using renewable power	Australia North Africa	Japan Europe	LH_2, LOHC (toluene)

The import and export locations differ from analysis to analysis. Shipping from Australia to Japan and from North Africa to Europe is considered by the International Energy Agency (IEA) [17]. The large-scale analysis by Roland Berger [7] focuses on the route from Arabian Gulf to Rotterdam. Japan is the import terminal assumed by Song et al. [8], Gallardo et al. [9], Wijayanta et al. [14] and Ishimoto et al. [16] because of the large hydrogen demand within the Japanese strategy to achieve net-zero greenhouse gas emissions by 2050 [18]. The export terminals of these evaluations are located in different countries: Song et al. [8] consider hydrogen produced by offshore wind farms in China, Gallardo et al. [9] by solar parks in Chile, Wijayanta et al. [14] analyze Australia as an export terminal, while Ishimoto et al. [16] focus on Norway. The Scandinavian region is considered because, apart from a high wind availability, it is rich in natural gas. Indeed, the study evaluates to blend hydrogen produced by renewable sources and by natural gas coupled with carbon capture and storage. The previous list of shipping and receiving terminals highlights that the ammonia production sites are located in renewable energy-rich areas, while importing regions are countries with high hydrogen demand but lack ~~of~~ green energy sources. Papadias et al. [12] and Wood [11] evaluate the ammonia value chain considering hydrogen production from natural gas. The steps of the value chain are independent of the hydrogen source considered. However, the application of non-green hydrogen may influence the location of the export sites, e.g. Papadias et al. [12] consider the US Gulf Coast due to the low price of natural gas.

The cracking of ammonia to hydrogen is the final stage of the value chain. Centralized cracking is considered when the reconversion takes place in a single hub [7-9, 11, 12, 16]. On the other hand, the decentralized application involves implementing small-scale cracking units at some end users. The small-scale analysis by Roland Berger [7] assumes 14 cracking plants, located at the end users, while IEA [17] studies decentralized cracking at the hydrogen refueling stations.

In summary, a lot of research activity is ongoing regarding hydrogen transportation in the form of liquefied ammonia. However, none of them involves cost estimation by simulating the cost-driving processes: ammonia synthesis starting from green hydrogen and ammonia cracking on a large- or small-scale.

The purpose of this article is to carry out a techno-economic assessment of green hydrogen transportation in the form of liquefied ammonia from North Africa to Italy. The cost-driving processes of the value chain are

simulated through the Aspen Plus® V.11 [19] commercial software simulator. The obtained material and energy balances are used to evaluate the investment and operating costs of the process plants. Two alternative options for the destination of the hydrogen delivered are investigated: a H_2 valley, where all the hydrogen is conveyed for its end use in the industrial sector, and refueling stations to serve the mobility sector.

2. Basis of design

In the present work, green hydrogen transport from a hypothetical renewable electricity hub located in North Africa to a hypothetical utilization site located inland 100 km from a European port is considered, with a sea distance of about 2500 km. Hydrogen is available at a constant flow rate of 20000 Nm^3/h, a pressure of 20 bar and a temperature of 25 °C. It is supposed to be produced by a 100 MW electrolyzer, powered by a solar photovoltaic plant. The transport of hydrogen in the form of liquefied ammonia is considered. The system boundaries are from the carrier synthesis starting from green hydrogen, whose production is not included, to hydrogen supply before end use. Two options for the destination of the hydrogen delivered are investigated: a H_2 valley, operated at 30 bar, where all the hydrogen is conveyed for its end use in the industrial sector (required H_2 purity of 99.9 mol%), and H_2 Refueling Stations (HRS), with a 500 kg/d H_2 demand each, to serve the mobility sector (required H_2 purity of 99.97 mol%, according to standard ISO 14687:2019 Hydrogen fuel quality - Product specification). The pressure of the H_2 delivered to the HRS is 15 bar. The compression required to fill the car tanks, typically at 350/700 bar, is outside the system boundaries. The value chain consists of ammonia synthesis, storage at the loading terminal, maritime transport, storage at the unloading terminal, distribution, storage at the end user/users, ammonia cracking. In the case of hydrogen delivery to HRS two possibilities for ammonia cracking are considered: decentralized cracking at the end users, with upstream distribution of liquefied ammonia, and centralized cracking at the port of arrival, with downstream distribution of compressed gaseous hydrogen. The amount of H_2 delivered differs between the investigated options because of different ammonia consumption of the cracking process.
Due to the significant inflation for the year 2022, two different scenarios are analyzed: a "present" scenario, which takes into account the current cost of utilities, and a "future" scenario, which considers the expected decrease in prices over the next 4 years.

3. Methodology of techno-economic assessment

The Levelized Cost of Hydrogen Transport (*LCoHT*) [20], which is computed according to Eq.(1), is used to assess the H_2 transport cost, overall and for each step of the value chain, as defined in Section 2, for the investigated cases.

$$LCoHT = \frac{\sum_{t=0}^{N-1} \frac{CAPEX_t + OPEX_t}{(1+WACC)^t}}{\sum_{t=0}^{N-1} \frac{P_{H_2,out}}{(1+WACC)^t}} \quad (1)$$

In Eq.(1), $P_{H2,out}$ is the annual amount of hydrogen delivered, *WACC* is the weighted average cost of capital, *t* is the year (where *t*=0 is the current year and *N-1* is the end year), $CAPEX_t$ and $OPEX_t$ are the capital and operating expenditures, respectively, at time *t*. Table 2 reports the financial assumptions.

Table 2 – Financial assumptions.

Item	Value
WACC	5%
Base year (*t*=0)	2022
Project lifetime	25 y
Construction period	3 y (*CAPEX* breakdown: 40%, 30%, 30%)
Decommission cost	5% *CAPEX* [21]
Plant availability (H_{eq})	8000 h/y
Exchange rate (2022)	0.951 €/US-$ [22]

3.1 Cost-driving processes

The economic assessment of the cost-driving processes, ammonia synthesis and cracking, is performed according to the Turton methodology [23]. This methodology allows a rough estimate of the plant costs and has to be intended as a preliminary feasibility study. The capital expenditures (*CAPEX*) of the plant are calculated according to the Guthrie method [24]. It provides, for each piece of equipment, the calculation of the purchased base cost $C_{p,i}^0$, through the equation:

$$\log_{10}\left(C_{p,i}^0(2001)\right) = K_{1,i} + K_{2,i}\log_{10}(A_i) + K_{3,i}\left[\log_{10}(A_i)\right]^2 \quad (2)$$

where A_i is the capacity or size parameter, specific to the type of equipment. The constants $K_{1,i}$, $K_{2,i}$ and $K_{3,i}$ to be used in Eq.(2) are available in [23] and allow to evaluate the cost of the equipment referred to the year 2001. To obtain an estimate at the present time, this cost must be updated taking into account economic inflation. This can be done by considering the following expression:

$$C_2 = C_1\left(\frac{I_2}{I_1}\right) \quad (3)$$

where *C* is the purchased cost, *I* a cost index and the subscripts refer to different times. The cost index used in this analysis is the Chemical Engineering Plant Cost Index (*CEPCI*), which is $CEPCI_{2001}$ = 397 and $CEPCI_{2022}$ = 816.5.

To take into account the effect on the cost of the equipment of the construction material and the operating pressure, the bare module cost ($C_{BM,i}$) is introduced, which is calculated as:

$$C_{BM,i} = C_{p,i}^0 F_{BM,i} = C_{p,i}^0\left(B_{1,i} + B_{2,i}F_{M,i}F_{P,i}\right) \quad (4)$$

where $F_{BM,i}$ (bare module factor) is a function of the parameters $F_{M,i}$ (material factor), which depends on the material of construction, and $F_{P,i}$ (pressure factor), which considers the operating pressure of the equipment. The values of the constants $B_{1,i}$ and $B_{2,i}$, tabulated for each equipment i, are available in [23].

The bare module cost for carbon steel construction material and atmospheric operating pressure, $C^0_{BM,i}$, and the bare module factor for the equipment under these conditions, $F^0_{BM,i}$, are calculated by setting $F_M = F_P = 1$.

Starting from the bare module cost for the equipment, the total module cost (C_{TM}) is calculated with equation (5), which takes into account an increase of 18% for contingency costs and fees. The *CAPEX*, as in Eq.(6), consider the cost for site development, auxiliary buildings, off-sites and utilities (grassroots cost) by suitably increasing the total module cost.

$$C_{TM} = 1.18 \sum_{i=1}^{n} C_{BM,i} \tag{5}$$

$$CAPEX = C_{TM} + 0.5 \sum_{i=1}^{n} C^0_{BM,i} \tag{6}$$

The following additional assumptions are introduced for the evaluation of *CAPEX*:

- for the ammonia synthesis section, the investment cost associated with the initial loading of the refrigerant in the closed cycle, used to liquefy the ammonia, is neglected, considering that it is much lower than the cost for the refrigeration cycle equipment;
- for the cracking section, in both the centralized and decentralized applications, the cost of the cracking unit is retrieved from the literature, to provide a reasonably accurate estimate. In particular, the cost function reported by Cesaro et al. [25] is used for the centralized application, while for the decentralized application (small-scale crackers) the estimate suggested by Thermal Dynamix™ [26], which is responsible for marketing such equipment, is introduced. Furthermore, the investment cost associated with the Pressure Swing Adsorption (PSA) units for the separation of the unconverted ammonia and the nitrogen co-produced from the hydrogen is neglected, considering that it is significantly lower compared to the cost of the cracker [27].

The operating expenditures (*OPEX*) are the costs associated with the daily operation of a chemical plant and, according to Turton et al. [23], they are computed as the sum of different cost items, related to three main cost categories: Direct Manufacturing Costs (*DMC*), which consist of the operating expenses varying with the production rate, Fixed Manufacturing Costs (*FMC*), which are not influenced at all by changes in the production level and they include property taxes, insurance and plant overhead costs, and General Expenses (*GE*), which rarely vary with the production rate and they include management, sales, financing and research functions.

The *OPEX* estimation requires that the following costs are known or at least can be estimated: *CAPEX*, cost of raw materials (C_{RM}), cost of utilities (C_{UT}), cost of operating labor (C_{OL}) and cost of waste treatment (C_{WT}). Factors for estimating the other cost items are given in Table 4.

C_{RM} accounts for the costs of chemical feedstocks required by the process. They are assumed to be negligible in the present analysis since the only feedstock is the green hydrogen, but its production cost must not be considered because out of the system boundaries, as stated in Section 2. C_{UT} involves the costs associated to the consumption of fuel, electricity, steam, cooling water (CW) and refrigerated water (RW). The specific utility costs utilized in the present analysis for the "present" and "future" scenarios are reported in Table 3. The utility consumption is calculated through the energy balance retrieved from process simulations.

Table 3 – Specific utility costs for the "present" and "future" scenarios [28].

Utility	Units	"present"	"future"
Electricity	€/MWh	500	220
CW (30 to 40 °C)	€/GJ	0.3583	0.3583
RW (15 to 25 °C)	€/GJ	32.3408	14.4768

C_{OL} is the cost of personnel required for plant operations. It depends on the number of operators per shift, N_{OL}, computed with Eq. (7), as suggested by Turton et al. [23], and on the average yearly operator wage, assumed to be 12000 € and 35300 € respectively for North African and Italian workers (values taken from [29] as the average salary of a chemical plant operator in Algeria and Italy, respectively), considering that a single operator works on the average 45 weeks a year, five 8-hour shifts a week.

$$N_{OL} = \text{round up}\left[\left(6.29 + 31.7 \cdot P^2 + 0.23 \cdot N_{np}\right)^{0.5}\right] \quad (7)$$

where P is the number of units involving solid particulate management (e.g. transport and distribution, particle size control), and N_{np} is the number of units handling fluids (excluding valves and pumps).

The cost of waste treatment (C_{WT}) is neglected in the present analysis.

Table 4 – Estimation of operating costs according to the Turton methodology [23].

Cost item	Calculated as
Direct Manufacturing Costs (DMC)	
Raw Materials (C_{RM})	neglected
Utilities (C_{UT})	
Operating labor (C_{OL})	
Waste treatment (C_{WT})	neglected
Direct supervisory and clerical labor	$0.18 \cdot C_{OL}$
Maintenance and repairs	$0.06 \cdot CAPEX$
Operating supplies	$0.009 \cdot CAPEX$
Laboratory charges	$0.15 \cdot C_{OL}$
Patents and royalties	$0.03 \cdot OPEX$
Total DMC	$C_{UT} + 1.33 \cdot C_{OL} + 0.069 \cdot CAPEX + 0.03 \cdot OPEX$
Fixed Manufacturing Costs (FCM)	
Local taxes and insurance	$0.032 \cdot CAPEX$
Plant overhead costs	$0.708 \cdot C_{OL} + 0.036 \cdot CAPEX$
Total FMC	$0.708 \cdot C_{OL} + 0.068 \cdot CAPEX$
General Expenses (GE)	
Administration costs	$0.177 \cdot C_{OL} + 0.009 \cdot CAPEX$
Distribution and selling costs	$0.11 \cdot OPEX$
Research and development	$0.05 \cdot OPEX$
Contingency	$0.05 \cdot OPEX$
Total GE	$0.177 \cdot C_{OL} + 0.009 \cdot CAPEX + 0.21 \cdot OPEX$
Total OPEX (DMC+FMC+GE)	$C_{UT} + 2.215 \cdot C_{OL} + 0.24 \cdot OPEX + 0.146 \cdot CAPEX$

3.2 Maritime transport

For the maritime transport of the liquefied ammonia, the *CAPEX* related to the purchase of the ship and the *OPEX* related to the labor, fuel, CO_2 emissions, maintenance and insurance are considered.

It is assumed to buy one ship, whose capacity is calculated on the basis of the number of days in which the carrier must be stored ($t_{\text{prod. to store}}$) defined as:

$$t_{\text{prod. to store}} = 2 \cdot t_{\text{one-way trip}} + t_{\text{loading and unloading}} + t_{\text{safety margin}} \quad (8)$$

where $t_{one\text{-}way\ trip}$ is the number of days for the one-way trip, $t_{\text{loading and unloading}}$ is the number of days required for loading and unloading the vessel, assumed to be equal to 1 day, and $t_{\text{safety margin}}$ is the time deemed reasonable to cover any delays, assumed to be 2 days. Considering a vessel speed of 16 knots (about 30 km/h), the $t_{\text{prod. to store}}$ is about 10 days.

The gross capacity of the ship (V_{ship} [m^3] in Eq.(9)) is computed considering that it is possible to use a maximum of 98% of the capacity for safety reasons and that a certain amount of residue, assumed equal to 4% by volume as for the LNG tanks [30], must remain in the tanks in order to cool them.

$$V_{\text{ship}} = \frac{P_{H_2} \cdot t_{\text{prod. to store}}}{\rho_{\text{NH}_3} \cdot (0.98 - 0.04)} \quad (9)$$

In Eq.(9) P_{H2} [kg/d] is the green hydrogen productivity and ρ_{NH3} is the volumetric density of liquid ammonia, equal to 677 kg/m^3.

The investment costs associated with the ship are retrieved from case studies for liquefied ammonia/liquefied petroleum gas (LPG) available in the literature and reported in Table 5. They are inflation-adjusted to the year 2022 using the *CEPCI* and interpolated using a power law to get the investment cost as a function of the gross capacity of the ship.

Table 5 – Gross capacity of the ship (V_{ship} [m^3]), reference year and *CAPEX* [M$] together with the literature source.

Source	V_{ship} [m^3]	Reference year	Reference *CAPEX* [M$]
Danish ship finance [31]	35000	2020	41
Danish ship finance [31]	15000	2020	36
Intermodal [32]	25000	2022	52
Golden Destiny [33]	22000	2022	55
Golden Destiny [34]	5500	2021	20

The labor cost ($OPEX_{\text{labor}}$ [M€/y] in Eq.(10)) is calculated by considering a crew size (*Crew* in Eq.(10)) of 16 people, as reported in the technical data sheet of a vessel with almost the same capacity as the one considered in this study [35]. It is assumed that two complete crews alternate in one year and that the single operator has a yearly wage (C_{labor} in Eq.(10)) of 52000 €/y.

$$OPEX_{\text{labor}} = C_{\text{labor}} \cdot Crew \cdot 2 \cdot 10^{-6} \quad (10)$$

Ships are assumed to be propelled by a traditional fuel engine such as IFO 380. The cost of this fuel (C_{fuel} in Eq.(11)) is assumed to be 580 €/t in the "present" scenario and 450 €/t in the "future" scenario. The fuel consumption ($Cons_{\text{fuel}}$ in Eq.(11)) is assumed equal to 13 t/d, as reported in the technical data sheet previously

considered [35]. Thus, the operating cost associated with fuel consumption ($OPEX_{fuel}$ [M€/y] in Eq.(11)) is calculated as:

$$OPEX_{fuel} = C_{fuel} \cdot Cons_{fuel} \cdot \frac{2 \cdot t_{one\text{-}way\ trip}}{t_{prod.\ to\ store}} \cdot \frac{H_{eq}}{24} \cdot 10^{-6} \quad (11)$$

The operating cost associated with CO_2 emissions ($OPEX_{CO2}$ [M€/y] in Eq.(12)) is calculated assuming a cost of CO_2 emissions (C_{CO2} in Eq.(12)) of 90 €/t in the "present" scenario and 105 €/t in the "future" scenario, and a value for the specific CO_2 emissions per volume of IFO 380 (e_{fuel} in Eq.(13)) equal to 11.24 $kg_{CO2}/gallon_{IFO\ 380}$ [36]:

$$OPEX_{CO_2} = E_{fuel} \cdot C_{CO_2} \cdot \frac{2 \cdot t_{one\text{-}way\ trip}}{t_{prod.\ to\ store}} \cdot \frac{H_{eq}}{24} \cdot 10^{-6} \quad (12)$$

where E_{fuel} [t/d] is the CO_2 emissions rate, calculated as:

$$E_{fuel} = \frac{Cons_{fuel} \cdot e_{fuel} \cdot 264.2\left[\text{gallon}/\text{m}^3\right]}{\rho_{IFO\ 380}} \quad (13)$$

where $\rho_{IFO\ 380}$ is the volumetric density of IFO 380, equal to 990 kg/m^3.

The costs related to maintenance and insurance are accounted as 10% of the *CAPEX* [23].

During sea transport, a quantity of ammonia equal to 0.1%/d is lost due to the boil-off phenomenon. In principle, the boil-off gas can be reliquefied or used for power generation on board, but, in this analysis, it is assumed not to recover its value.

3.3 Storage

Liquefied ammonia is usually stored at about -30 °C and at a pressure slightly above the atmospheric one, 1.3 bar, inside spherical tanks (minimum area/volume ratio) equipped with polyurethane foam insulation to limit losses due to the boil-off phenomenon.

For the storage of the liquefied ammonia, only the *CAPEX* related to the purchase of the storage tank are considered. The *OPEX* are related to maintenance and insurance and are accounted as 10% of the *CAPEX*. The boil-off losses are assumed to be negligible. In fact, it is possible to reliquefy the boil-off gas at the loading terminal and to send it to the cracking process at the site where reconversion occurs.

The investment costs associated with the tank are retrieved from literature and reported in Table 6. They are inflation-adjusted to 2022 using the *CEPCI* index and interpolated using a power law to get the investment cost as a function of the gross capacity of the tank.

Table 6 – Gross capacity of the tank (V_{tank} [m^3]), reference year and *CAPEX* [M$] together with the literature source.

Reference	V_{tank} [m^3]	Reference year	Reference *CAPEX* [M$]
Sadler et al. [5]	81536	2020	32
Bartels and Pate [37]	36898	2007	20.2
Olson [38]	29518	2012	20

Leighty [39]	44277	2010	15

For each full-capacity terminal (port of departure, port of arrival and H_2 valley), the purchase of a tank is assumed, the gross capacity of which (V_{tank} [m^3] in Eq.(14)) is calculated considering the storage of the volume transported by the ship V_{ship} increased by 10% as a safety margin to take into account any delay.

$$V_{tank} = (1+0.1) \cdot V_{ship} \tag{14}$$

In the case of decentralized cracking at the HRS, the purchase of a liquefied ammonia tank with a capacity of 5.2 m^3 is assumed for each of them, whose *CAPEX* are estimated to be 0.068 M€ (value retrieved from [40], inflation-adjusted to 2022 and scaled for the capacity using the six tenths rule).

3.4 Distribution

For the distribution of the liquefied ammonia, the *CAPEX* related to the purchase of the trucks and the *OPEX* related to the labor, fuel, CO_2 emissions, maintenance and insurance are considered.

The number of trucks to buy n_{trucks} is calculated considering that each truck makes 2 round trips per day:

$$n_{trucks} = \text{round up}\left(\frac{V_{\text{unloaded from the ship}}}{V_{truck} \cdot t_{\text{prod. to store}} \cdot 2} \right) \tag{15}$$

where V_{truck} [m^3] is the net capacity of a single truck, $V_{\text{unloaded from the ship}}$ [m^3] is the volume of the hydrogen carrier unloaded from the ship at the port of arrival and is calculated taking into account that part of the volume initially loaded is lost due to the boil-off phenomenon with a rate (r_{BOG} in Eq.(16)) of 0.1 %/d:

$$V_{\text{unloaded from the ship}} = \frac{P_{H_2} \cdot t_{\text{prod. to store}}}{\rho_{NH_3}} \cdot (1 - r_{BOG})^{t_{\text{one-way trip}}} \tag{16}$$

The distribution can take place upstream or downstream of the cracking process. In the first case, liquefied ammonia would be distributed by trucks and cracking would take place *in situ*. In the second case, gaseous hydrogen would be distributed by trucks, after being compressed to increase its density and stored in suitable cylindrical tanks (tube trailers).

Trucks consist of two major units: the tractor unit with the driver's cab and a trailer that mounts the tractor. The same tractor unit is considered for both liquefied ammonia and compressed hydrogen trucks, having an investment cost of 0.24 M€ (value retrieved from [40], inflation-adjusted to 2022). A liquefied ammonia trailer with a net capacity V_{truck} of 20 m^3 (13650 kg) has an investment cost of 0.16 M€ (value retrieved from [40], inflation-adjusted to 2022), while a compressed gas trailer with a net capacity of 500 kg has an investment cost of 0.70 M€ (value retrieved from [41], inflation-adjusted to 2022). A truck lifetime of 12 years is assumed.

The labor operating cost ($OPEX_{labor}$ [M€/y] in Eq. (17)) is calculated considering that the number of drivers per shift is equal to the number of trucks and that the single operator has a yearly wage (C_{labor} in Eq. (17)) of 17600 €/y (value taken from [29] as the Italian average salary of a tanker truck driver), and works 45 weeks a year, five 8-hour shifts a week.

$$OPEX_{\text{labor}} = C_{\text{labor}} \cdot n_{\text{trucks}} \cdot \frac{H_{\text{eq}}}{45 \cdot 5 \cdot 8} \cdot 10^{-6} \quad (17)$$

Trucks are assumed to have a diesel engine and consume $Cons_{\text{fuel}}$ = 35 L/100 km [41]. Thus, the operating cost associated with fuel consumption ($OPEX_{\text{fuel}}$ [M€/y] in Eq.(18)) is calculated as:

$$OPEX_{\text{fuel}} = C_{\text{fuel}} \cdot Cons_{\text{fuel}} \cdot d \cdot 2 \cdot \frac{V_{\text{unloaded from the ship}}}{V_{\text{truck}} \cdot t_{\text{prod. to store}}} \cdot \frac{H_{\text{eq}}}{24} \cdot 10^{-6} \quad (18)$$

where d is the distance between the port and the end user (100 km) and C_{fuel} is the diesel cost, assumed equal to 1.8155 €/L (average price of diesel in Italy in 2022) for both the "present" and "future" scenarios. The cost of CO_2 emissions is calculated considering that diesel has specific CO_2 emissions (e_{fuel} in Eq.(19)) equal to 10.19 $kg_{CO2}/gallon_{diesel}$ [36].

$$OPEX_{CO_2} = C_{CO_2} \cdot E_{\text{fuel}} \cdot d \cdot 2 \cdot \frac{V_{\text{unloaded from the ship}}}{V_{\text{truck}} \cdot t_{\text{prod. to store}}} \cdot \frac{H_{\text{eq}}}{24} \cdot 10^{-6} \quad (19)$$

where E_{fuel} [t/km] is calculated as:

$$E_{\text{fuel}} = Cons_{\text{fuel}} \cdot e_{\text{fuel}} \cdot 264.2\left[\text{gallon}/\text{m}^3\right] \cdot 10^{-6} \quad (20)$$

The costs related to maintenance and insurance are accounted as 10% of the *CAPEX*.

4. Simulation of the cost-driving processes

The cost-driving processes of the value chain are ammonia synthesis and cracking. Therefore, simulation of these processes is carried out with the aim of computing material and energy balances, useful for the economic evaluation, as described in Section 3.1.

The ammonia synthesis process starting from green H_2 and nitrogen separated from air is the first block of the value chain in all the investigated cases. The plant size is set by the green hydrogen input flowrate and, hence, is smaller compared to conventional fossil-based ammonia synthesis plants.

If the destination of the produced hydrogen is a H_2 valley, centralized cracking of ammonia is performed at the valley, after the road transport of ammonia from the destination port to the valley itself. In the case of destinating the produced hydrogen to some HRS, each with 500 kg/d H_2 demand, two possible alternatives are identified for the reconversion of ammonia to gaseous hydrogen:

- centralized reconversion of NH_3 to hydrogen at the destination port. In this case, the produced hydrogen is compressed and distributed by trucks, operating at 250 bar, to all the HRS.
- decentralized reconversion of NH_3 to hydrogen at the H_2 Refueling Stations. In this case, the ammonia stored at the destination port is distributed by trucks to all the HRS, where it is converted into gaseous hydrogen.

4.1 Ammonia synthesis and liquefaction

To carry out the synthesis of NH_3 and, ultimately, to estimate the capital and operating costs associated with this block of the chain, it is necessary to provide a nitrogen feed to the process. Therefore, the production of nitrogen (N_2) from air is considered, rather than introducing a complete air separation unit (ASU), since a possible end use of the oxygen (O_2) produced is not conceived in the process. In the literature, several schemes are available for the production of N_2 from air. In particular, the Air Products scheme proposed by Agrawal and Thorogood [42] is selected and simulated in Aspen Plus® V11 [19] to get material and energy balances.

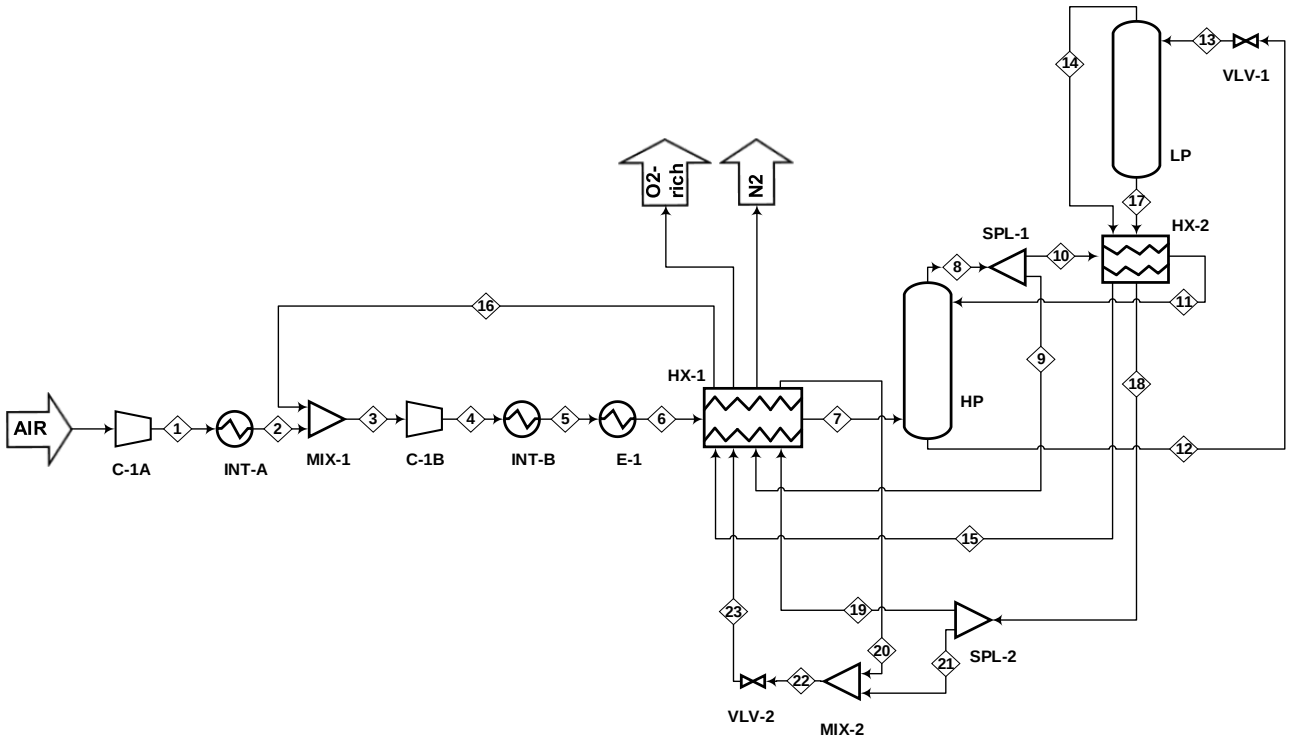

Fig. 2 – Process scheme of nitrogen production from air.

The process, depicted in Fig. 2, involves the separation of air, compressed to 8.5 bar in C-1A and C1-B and pre-cooled to its dew point in the main exchanger (HX-1), via cryogenic distillation. The fed air is sent to the rectifying section of the distillation column (HP), operating at high pressure (P = 8 bar) and made up of 50 theoretical trays, to be separated into a vapor phase overhead product, consisting of pure nitrogen (residual O_2 content of few ppm), and in a bottom product, consisting of an approximately equimolar mixture of O_2 and N_2. This mixture is fed, after expansion to 3 bar, to the stripping section of the distillation column (LP). At the top, a stream with composition close to that of air is obtained and it is recycled back to the second compression stage C-1B, after passing into HX-1 to cool the feed mixture. At the bottom, an oxygen-rich stream is separated and sent to HX-1 to cool the hot stream. The cooling duty necessary to condense part of the top product of the HP column, which constitutes the reflux of the column itself, is provided by the evaporation of the bottom product of the LP column. The process is autothermal: the power required for the separation is all provided by the air compressors. The nitrogen stream thus produced is the feed for the ammonia synthesis stage.

Table 7 reports the inlet and outlet streams specifications for the nitrogen production process in Fig. 2.

Table 7 – Inlet and outlet streams specifications at the battery limits for the process in Fig. 2.

Stream		AIR	N2	O2-rich
T	**[°C]**	25	24.3	24.3
P	**[bara]**	1.01	8.04	3.05
molar fractions				
O_2		0.2100	0.0000	0.5757
N_2		0.7900	1.0000	0.4243
F_{TOT}	**[kmol/h]**	468.57	297.64	170.93

The energy balance of the process is reported in Table 8 and Table 9, in terms of cooling duties and electric power consumptions, respectively.

Table 8 – Cooling duties, together with the corresponding utility, of the process in Fig. 2.

Equipment	T_{IN} [°C]	T_{OUT} [°C]	Q [kW]	utility
INT-A	164.96	40	479.34	CW
INT-B	161.58	40	687.11	CW
E-1	40	25	84.81	RW

Table 9 – Electric power consumption of the process in Fig. 2.

Equipment	P_{IN} [bara]	P_{OUT} [bara]	W [kW]
C-1A	1.01	3.12	534.89
C-1B	3.12	8.5	709.35

The Haber-Bosch ammonia synthesis process is widely established and applied on a large-scale. The process is based on reaction (21) and is usually catalyzed by iron-based catalysts.

$$N_2 + 3H_2 \rightarrow 2NH_3 \tag{21}$$

To simulate the ammonia synthesis section in Aspen Plus® V11 [19] and, hence, estimate its costs, reference is made to the template available in the process simulator for ammonia synthesis from fossil sources, modifying it significantly both to remove the steam reforming section and to adapt it to the different capacity (different sizes of reaction modules). In this template, the routines developed by Mok [43] for describing the Nielsen kinetic model [44] (Eq.(22) with R [kmol/(h·m^3)]) are implemented.

$$R = A_c \frac{AK\left(a_N k_{eq}^2 - \frac{a_A^2}{a_H^3}\right)}{\left(1 + K_a \frac{a_A}{a_H^w}\right)^{2\alpha}} \tag{22}$$

where:

- A_c is the catalyst activity, considered constant and equal to 0.4 for sake of simplicity;
- w = 1.523;
- α = 0.654;
- k_{eq} is the equilibrium constant, computed through Eq.(23) with T in [K];
- AK is calculated according to Eq.(24) with T in [K];
- K_a is calculated according to Eq.(25) with T in [K];
- a_N, a_H, a_A are the activities of nitrogen, hydrogen and ammonia, respectively.

$$\log_{10} k_{eq} = -2.691122 \log_{10}(T) - 5.519265 \cdot 10^{-5} T + 1.8488663 \cdot 10^{-7} T^2 + \frac{2001.6}{T} + 2.6899 \qquad (23)$$

$$AK = 3.945 \cdot 10^{10} \exp\left(-\frac{5622}{T}\right) \qquad (24)$$

$$K_a = 2.94 \cdot 10^{-4} \exp\left(\frac{12104}{T}\right) \qquad (25)$$

The reactor, consisting of 3 adiabatic beds with intercooling, operates at 200 bar and is suitably sized in order to minimize the residence time for each stage and, consequently, minimize the volume of catalyst needed. Downstream of the reaction section, the produced ammonia must be separated from the unreacted hydrogen and nitrogen, which have to be recycled back, while reaching the low temperature necessary for ammonia liquefaction at approximately ambient pressure.

The resulting process scheme is depicted in Fig. 3.

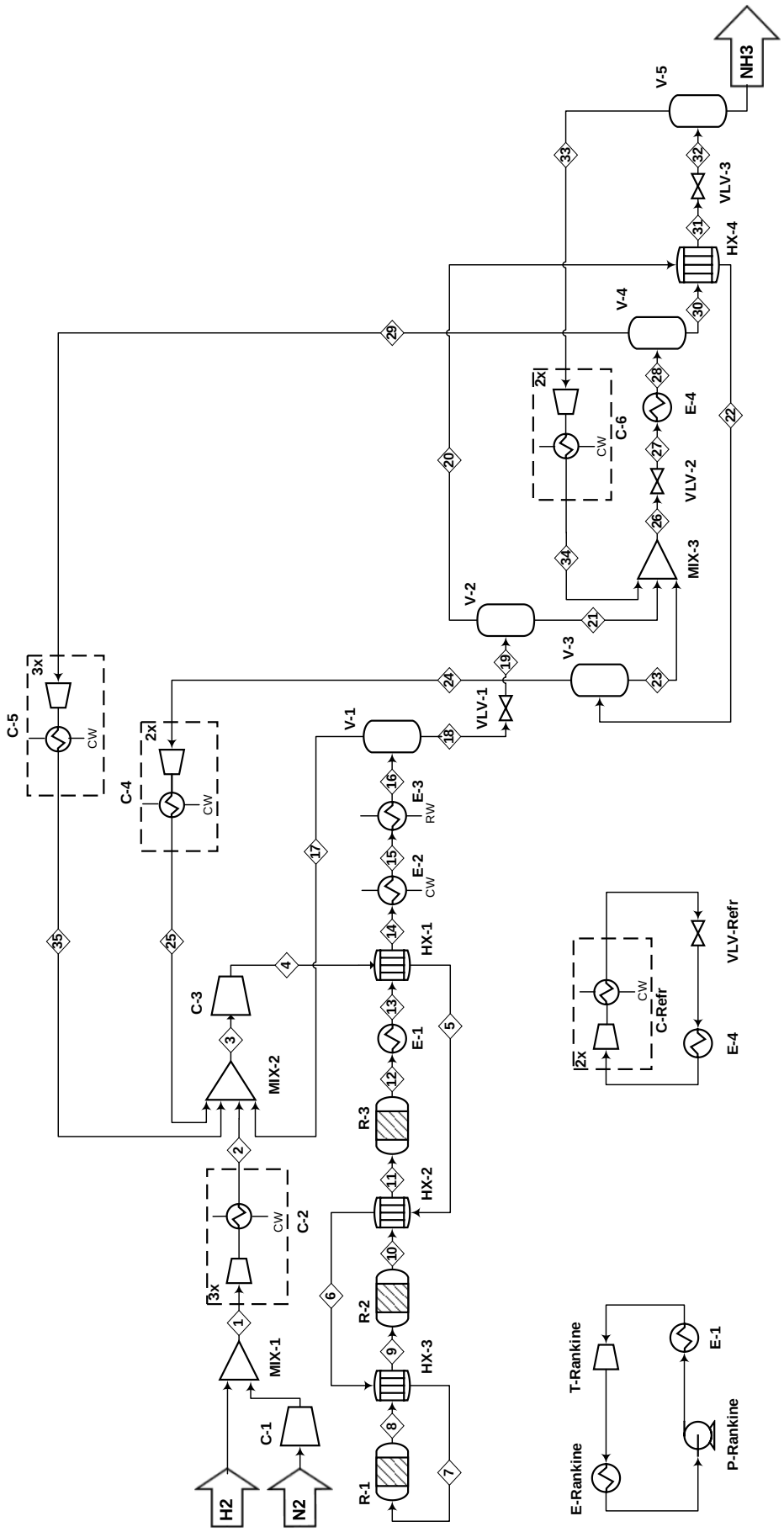

Fig. 3 – Process scheme of ammonia synthesis and liquefaction.

The nitrogen feed (N2 in Fig. 3), coming out from the air separation process illustrated in Fig. 2 at about 24 °C and 8 bar, is compressed to 20 bar and mixed with the hydrogen feed (H2 in Fig. 3). The resulting mixture is compressed to 193 bar in a three-stage compressor with intercooling (C-2 in Fig. 3). Downstream of the last post-cooler, the feed, at 40°C and 193 bar, is mixed with the recycled streams, the vapors leaving the separators V-2, V-3 and V-4, suitably compressed. The resulting stream is compressed to 200 bar in C-3 and heated to 347 °C through a series of process-process heat exchangers (HX-1, HX-2 and HX-3), which exploit the high enthalpy content of the products leaving the second and third reactor stages, before being sent to the first catalytic stage (R-1 in Fig. 3). The stream leaving the last reactor (R-3 in Fig. 3) contains, in addition to ammonia, hydrogen and nitrogen which must be separated and recycled back to the reaction stage. The goal is to obtain liquid ammonia at a pressure slightly higher than ambient pressure, with a purity higher than 99.95%. To reach the required specifications, the stream is first cooled in E-1 to 109 °C, supplying heat to a steam Rankine cycle for electricity generation, then, downstream HX-1, in E-2 and E-3, using cooling water and refrigerated water, respectively.

The biphasic stream leaving E-3 is separated in flash drum V-1: the vapor is recycled back to the reaction section, while the liquid is further purified in a series of flash drums operating at decreasing pressures. In particular, V-2 and V-3 operates at 30 bar, V-4 at 15 bar and V-5 at 1.3 bar (storage pressure). Cooling of the vapor from V-2 is obtained by heat exchange with the liquid from V-4 and is performed in order to condense ammonia, which is then separated in V-3, and avoid a recycle stream rich in the reaction product which would involve a shift of the synthesis reaction (Eq.(21)) toward the left. E-4 outlet temperature is set to -18 °C: in order to reach such a low temperature a refrigeration cycle, having ammonia as refrigerant, is used.

In Table 10 the inlet and outlet streams specifications are reported for the ammonia synthesis process in Fig. 3.

Table 10 – Inlet and outlet streams specifications at the battery limits for the process in Fig. 3.

Stream		**N2**	**H2**	**NH3**
T	**[°C]**	29.25	25	-28.98
P	**[bara]**	8.04	20	1.3
molar fractions				
H_2		0.0000	1.0000	0.0000
N_2		1.0000	0.0000	0.0000
NH_3		0.0000	0.0000	1.0000
F_{TOT}	**[kmol/h]**	297.64	892.91	595.27

The energy balance of the process is reported in Table 11 and Table ***12***, in terms of cooling duties and electric power consumptions, respectively.

Table 11 – Cooling duties, together with the corresponding utility, of the process in Fig. 3.

Equipment	T_{IN} **[°C]**	T_{OUT} **[°C]**	Q **[kW]**	**utility**
C-2 intercooler(1)	152.98	40	1101.30	CW
C-2 intercooler(2)	134.78	40	934.99	CW
C-2 intercooler(3)	135.17	40	957.88	CW
C-4 intercooler(1)	88.27	40	3.71	CW
C-4 intercooler(2**)**	155.73	40	9.23	CW
C-5 intercooler(1)	65.06	40	0.29	CW

C-5 intercooler(2)	143.59	40	1.24	CW
C-5 intercooler(3)	143.74	40	1.36	CW
C-6 intercooler(1)	73.48	40	8.39	CW
C-6 intercooler(2)	163.26	40	33.89	CW
E-2	66.66	40	2140.18	CW
E-3	40	25	925.15	RW
C-Refr intercooler(1)	142.41	40	163.85	CW
C-Refr intercooler(2)	159.99	40	988.48	CW
E-Rankine	49.98	49.98	6069.12	CW

Table 12 – Electric power consumption of the process in Fig. 3.

Equipment	P_{IN} **[bara]**	P_{OUT} **[bara]**	W **[kW]**
C-1	8.04	20	271.97
C-2	20	193	2889.49
C-3	193	200	126.92
C-4	30	193	16.32
C-5	15	193	3.40
C-6	1.3	15	53.14
C-Refr	1.5	16.32	352.07
P-Rankine	0.1	20	6.50
T-Rankine	20	0.1	-2013.25

4.2 Ammonia cracking

The dissociation of ammonia is a strongly endothermic process, described by reaction (26), that generally takes place at high temperatures, which represents the main drawback for application of the technology on an industrial scale.

$$2NH_3 \rightarrow N_2 + 3H_2 \tag{26}$$

As a result of the first studies and applications, and in parallel with the search for catalysts for thermal decomposition, alternative methods have been proposed in the literature to provide the required duty for activating the reaction. These methods include: application of electric current, electron beams or ions, microwaves, plasma or solar energy [45, 46].

In the present work, the simulations of centralized and decentralized cracking processes are developed assuming the application of thermocatalytic technology for the decomposition of ammonia into nitrogen and hydrogen on nickel-based catalyst.

Centralized cracking

In the case of centralized ammonia cracking, all the ammonia stored at the receiving terminal is converted into hydrogen. The centralized cracking process is simulated in Aspen Plus V11® [19] and its process scheme is shown in Fig. 4.

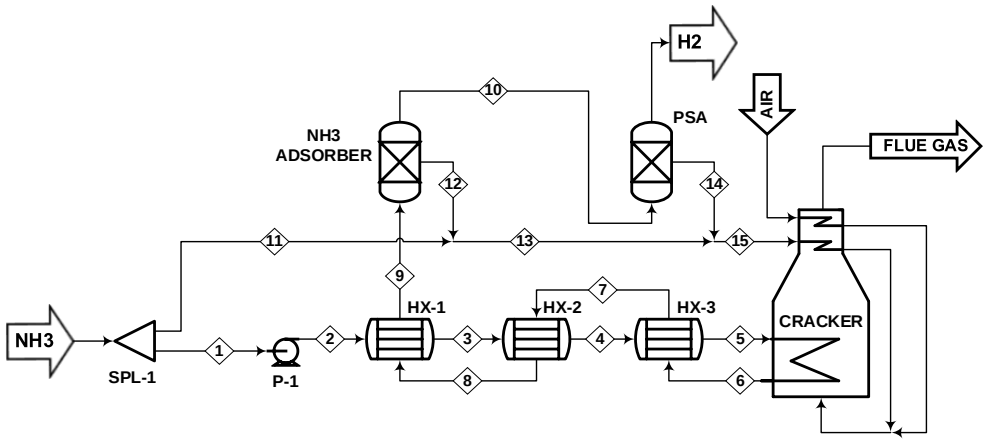

Fig. 4 – Process scheme of centralized ammonia cracking.

The ammonia stream (NH3 in Fig. 4) is pumped to 30 bar, preheated in a train of exchangers (HX-1, HX-2 and HX-3 in Fig. 4) exploiting the high enthalpic content of the reaction products and sent to the cracking reactor. The reactor, CRACKER in Fig. 4, is simulated with the RGibbs module of Aspen Plus® V11 [19] because no detailed kinetic data are currently available in the literature to build a reliable kinetic model. Therefore, the conversion of ammonia is that of thermodynamic equilibrium at the temperature and pressure of the reactor, i.e. 30 bar and 900°C. This temperature is in line with the operating conditions of commercially available nickel-based catalysts. The heat duty required for the cracking reaction is supplied by burning part of the fed ammonia, mixed with the waste streams with a high H_2 content leaving the purification section. Air is used as oxidizer in a quantity slightly exceeding the stoichiometric one, to ensure complete combustion.

Downstream of the reaction stage, the separation of the hydrogen product from the unconverted ammonia and nitrogen is performed via PSA. The outgoing hydrogen, H2 in Fig. 4, can then be distributed to the H_2 valley, its specifications being compatible with this application.

Table 13 reports the inlet and outlet streams specifications for the centralized cracking process in Fig. 4.

Table 13 – Inlet and outlet streams specifications at the battery limits for the process in Fig. 4.

Stream		**NH3**	**H2**	**AIR**	**FLUE GAS**
T	**[°C]**	-27.60	25.47	25	139.00
P	**[bara]**	1.3	30	1.01	1.01
molar fractions					
H_2		0.0000	0.9990	0.0000	0.0003
N_2		0.0000	0.0010	0.7900	0.7750
H_2O		0.0000	0.0000	0.0000	0.1910
NO		0.0000	0.0000	0.0000	0.0029
NH_3		1.0000	0.0000	0.0000	0.0000
N_2O		0.0000	0.0000	0.0000	0.0000
NO_2		0.0000	0.0000	0.0000	0.0000
O_2		0.0000	0.0000	0.2100	0.0309
F_{TOT}	**[kmol/h]**	592.33	698.07	608.13	999.28

The only utility in this process is electricity, which is used to drive the pump (P-1 in Fig. 4), and its consumption is 23.72 kW.

Decentralized cracking

The decentralized cracking process is simulated in Aspen Plus® V11 [19] and shown in Fig. 5.

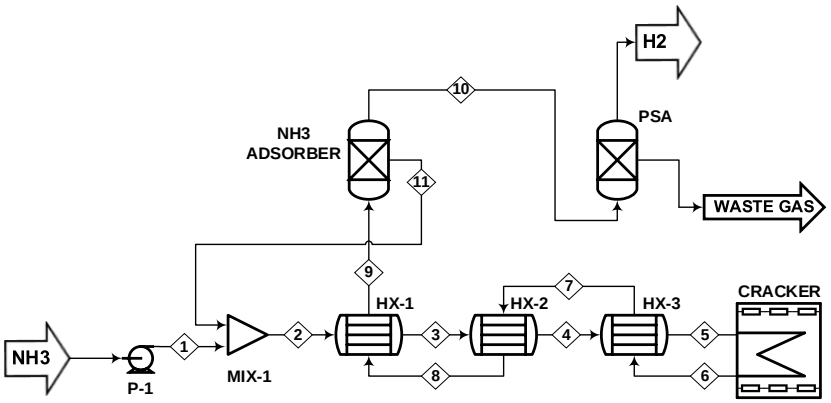

Fig. 5 – Process scheme of decentralized ammonia cracking.

The process is similar to what is reported in Fig. 4, except for the fact that the cracking reaction is powered by electricity, in line with commercially available small-scale ammonia crackers. Therefore, the combustion section for heat generation is not necessary. Downstream of the reaction stage, the separation of the hydrogen produced from nitrogen and unconverted ammonia is performed by adsorption. The separated nitrogen stream (WASTE GAS in Fig. 5), containing approximately 30% hydrogen on a molar basis, needs to be disposed of (for example, by flare combustion). The produced hydrogen, H2 in Fig. 5, can then be utilized to fill the car tanks operating at 350/700 bar, after being compressed at the HRS, since its specifications are compatible with this application.

In Table 14 the inlet and outlet streams specifications are reported for the decentralized cracking process in Fig. 5.

Table 14 – Inlet and outlet streams specifications at the battery limits for the process in Fig. 5.

Stream		**NH3**	**H2**	**WASTE GAS**
T	**[°C]**	-27.60	24.7	24.7
P	**[bara]**	1.3	30	30
molar fractions				
H_2		0.0000	0.9997	0.3105
N_2		0.0000	0.0003	0.6895
NH_3		1.0000	0.0000	0.000
F_{TOT}	**[kmol/h]**	8.07	10.29	5.85

Among the utilities necessary for the process, only electricity is considered to power the small-scale cracker and the pump (160.70 kW and 0.21 kW, respectively).

5. Results and discussion

The block flow diagram (BFD), together with the material balance along the entire value chain, is reported in Fig. 6a for the case of industrial end use of the hydrogen delivered, and in Fig. 6b for the case of hydrogen utilization in the mobility sector, considering both the alternatives of centralized and decentralized reconversion.

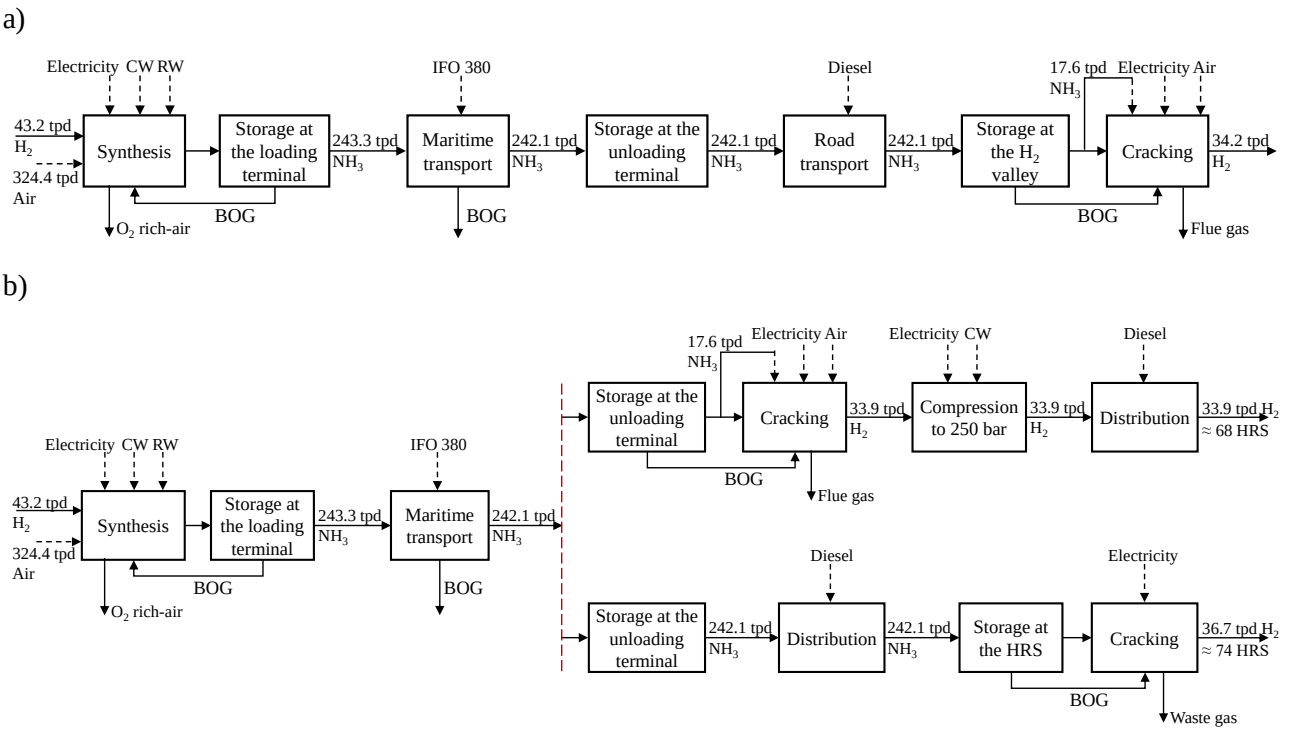

Fig. 6 – BFD of the liquefied ammonia value chain in the case of hydrogen destination to: a) a H_2 valley, b) Hydrogen Refueling Stations, for both the alternatives of centralized and decentralized reconversion.

In case of hydrogen delivery to a H_2 valley and to HRS with centralized reconversion, the carrier losses occur as boil-off during maritime transport and as fuel burned to sustain the endothermicity of the reaction in the cracking process. In case of H_2 destination to HRS with decentralized reconversion, carrier losses are only due to boil-off during shipping because the heat necessary for the cracking reaction is supplied by electrical resistances. Therefore, a higher number of refueling stations, about 74 in the latter case with respect to 68 in the former one, can be served.

The economic assessments carried out for the ammonia value chain are shown below, according to the methodology described in Section 3. The investment and operating costs for the ammonia synthesis and cracking processes are evaluated starting from the process simulations detailed in Section 0.

As regards the synthesis of ammonia (including the nitrogen separation section), the economic evaluation provides an investment cost of 91.12 M€. This value is in line with the results obtained by Morgan [47] for a plant of similar size to the one selected in this work. The *CAPEX* cost items are reported in Table 15, from which it is evident that almost all the investment costs for the synthesis process are due to the reactor, the heat exchangers and the compressors.

Table 15 – *CAPEX* [M€] for the ammonia synthesis process. In the Figure the breakdown of the C_{BM}.

	Equipment	***Cost* [M€]**
C_{BM}	Heat Exchangers	20.21
	Compressors	17.77
	Turbines	2.36

	Pumps	0.03	
	Columns	0.33	
	Vertical Vessels	1.94	
	Reactor	25.04	
C_{TM}		79.87	
CAPEX		91.12	

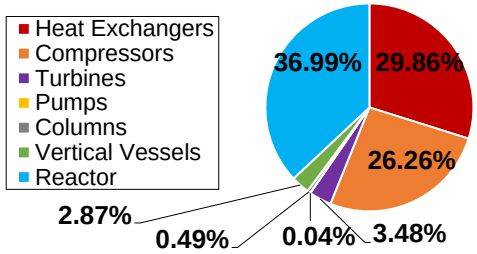

Operating costs, reported in Table 16, are equal to 35.33 M€/y and are mostly due to the cost of the electricity needed to drive the compressors.

Table 16 – *OPEX* [M€/y] for the ammonia synthesis process.

	***Cost* [M€/y]**
C_{UT}	12.88
C_{OL}	0.30
other DMC	7.45
FMC	6.41
GE	8.29
OPEX	35.33

As regards the centralized cracking of ammonia, the investment costs amount to 44.15 M€. The *CAPEX* cost items are reported in Table 17, from which it is possible to notice that almost all the investment costs are due to the cracker.

Table 17 – *CAPEX* [M€] for the centralized cracking process. In the Figure the breakdown of the C_{BM}.

	Equipment	***Cost* [M€]**	
C_{BM}	Heat Exchangers	1.27	
	Pumps	0.07	
	Cracker	25.14	
C_{TM}		31.25	
CAPEX		44.15	

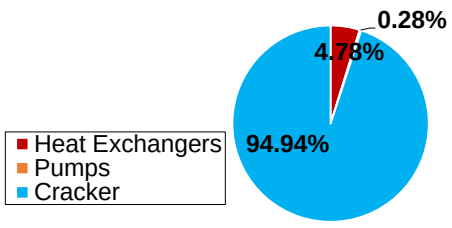

The operating costs of the centralized ammonia cracking process (Table 18) are equal to 10.15 M€/y. Among the utilities necessary for the process, only the electricity required by the pump to feed the ammonia to the process is considered, the cost of which is negligible. In this case, no external fuel is needed, since ammonia combustion with air is used to sustain the endothermicity of cracking reaction. In the performed economic

evaluation, the cost associated with the NO_x emissions due to the combustion reaction is neglected, assuming to reduce them with a non-catalytic process based on ammonia.

Table 18 – *OPEX* [M€/y] for the centralized cracking process.

	***Cost* [M€/y]**
C_{UT}	0.10
C_{OL}	0.53
other DMC	3.53
FMC	3.38
GE	2.62
OPEX	10.15

In the case of destinating the hydrogen to the Hydrogen Refueling Stations and reconverting the ammonia into hydrogen at the port, the above *CAPEX* and *OPEX* must be increased by the investment and operating costs associated with the compression of the gaseous hydrogen produced for its transport (at about 250 bar). These compression costs are equal to 9.72 M€ and 11.93 M€/y, respectively. Once H_2 reaches its destination, it must be unloaded from the trucks by lowering the pressure to 15 bar.

In the case of decentralized cracking at the HRS, the investment costs of the single unit dedicated to the production of 500 kg/d of H_2 are equal to 0.54 M€. The *CAPEX* cost items are reported in Table 19.

Table 19 – *CAPEX* [M€] for the decentralized cracking process. In the Figure the breakdown of the C_{BM}.

	Equipment	***Cost* [M€]**	
C_{BM}	Heat Exchangers	0.29	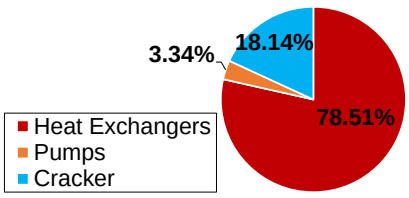
	Pumps	0.01	
	Cracker	0.07	
C_{TM}		0.43	
CAPEX		0.54	

The operating costs of the decentralized ammonia cracking process (Table 20) are equal to 1.21 M€/y for each of the HRS. Among the utilities necessary for the process, only electricity is considered to power the small-scale cracker and the pump. Again, no fuel is required. In the evaluations carried out, the cost related to the disposal of the nitrogen stream separated from the hydrogen produced by PSA (WASTE GAS in Fig. 5) is neglected, which cannot be emitted directly into the atmosphere due to the residual H_2 content.

Table 20 – *OPEX* [M€/y] for the decentralized cracking process.

	***Cost* [M€/y]**
C_{UT}	0.64
C_{OL}	0.09

other DMC	0.10
FMC	0.10
GE	0.27
OPEX	1.21

In addition to the cost drivers, to complete the techno-economic assessment of the value chain, the cost associated with maritime transport, storage and distribution to the end user is estimated.

The investment costs of transport by ship are related only to the purchase of the ship itself, having a capacity of 3900 m^3. The operating costs, on the other hand, are related to labor, fuel consumption, and CO_2 emission costs. The resulting *CAPEX* and *OPEX* for the maritime transport of liquefied ammonia are equal to 20.25 M€ and 6.25 M€/y, respectively.

In the case of hydrogen destination to a H_2 valley, three full-capacity storage tanks, one at the port of departure, one at the port of arrival and one at the H_2 valley, each with a capacity of 4200 m^3 need to be purchased. The overall *CAPEX* and *OPEX* result to be 30.59 M€ and 3.06 M€/y, respectively. In the case of hydrogen transport to HRS, two full-capacity tanks are required at the two ports, involving *CAPEX* and *OPEX* of 20.39 M€ and 2.04 M€/y, respectively. Moreover, if cracking is carried out at the HRS, a small-capacity liquefied ammonia tank is necessary to feed the process at each refueling station, adding overall *CAPEX* and *OPEX* of 4.96 M€ and 0.50 M€/y, respectively.

In the cases of hydrogen delivery to a H_2 valley and to HRS with cracking at the end users, liquefied ammonia is distributed, involving the purchase of 9 trucks. The overall *CAPEX* and *OPEX* are 3.57 M€ and 1.92 M€/y, respectively.

If, in the case of hydrogen delivery to HRS, the cracking of the ammonia is carried out at the port of arrival, compressed gaseous hydrogen must be distributed. In this case, 34 trucks need to be purchased, whose overall *CAPEX* and *OPEX* are 31.73 M€ and 9.10 M€/y, respectively.

The results in terms of *LCoHT* for each block of the value chain are reported in Fig. 7 for the case of hydrogen destined to the industrial sector and in Fig. 8 for the case of utilization in the mobility sector.

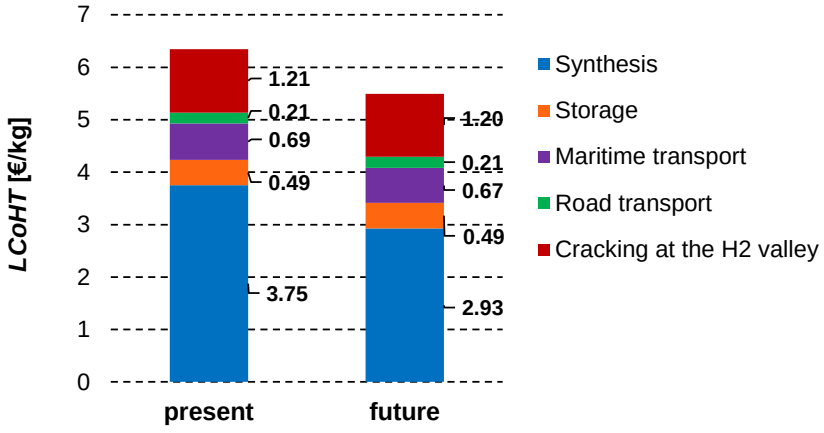

Fig. 7 – *LCoHT* [€/kg] in the case of hydrogen destination to a H_2 valley: comparison between the present and future scenarios.

The overall *LCoHT* is 6.34 €/kg in the "present" scenario, with an expected cost reduction to 5.49 €/kg in the "future" scenario. Looking at Fig. 7, it is possible to notice that the synthesis of ammonia starting from green hydrogen is the cost driver of the value chain, followed by the centralized cracking, while the storage, transport and distribution of the liquefied ammonia does not significantly influence the overall *LCoHT*. Furthermore, the infrastructure to move ammonia is already well established due to its widespread use and, hence, there are fewer opportunities for cost reduction.

In the future a reduction of the ammonia synthesis cost is foreseen due to the lower prices of the utilities, in particular electricity, exploited in the process. This trend is not observable for the ammonia cracking cost because the thermal power required by the cracking reactor, which is the most energy demanding equipment of the process, is provided by the combustion of part of the ammonia fed and not by external utilities.

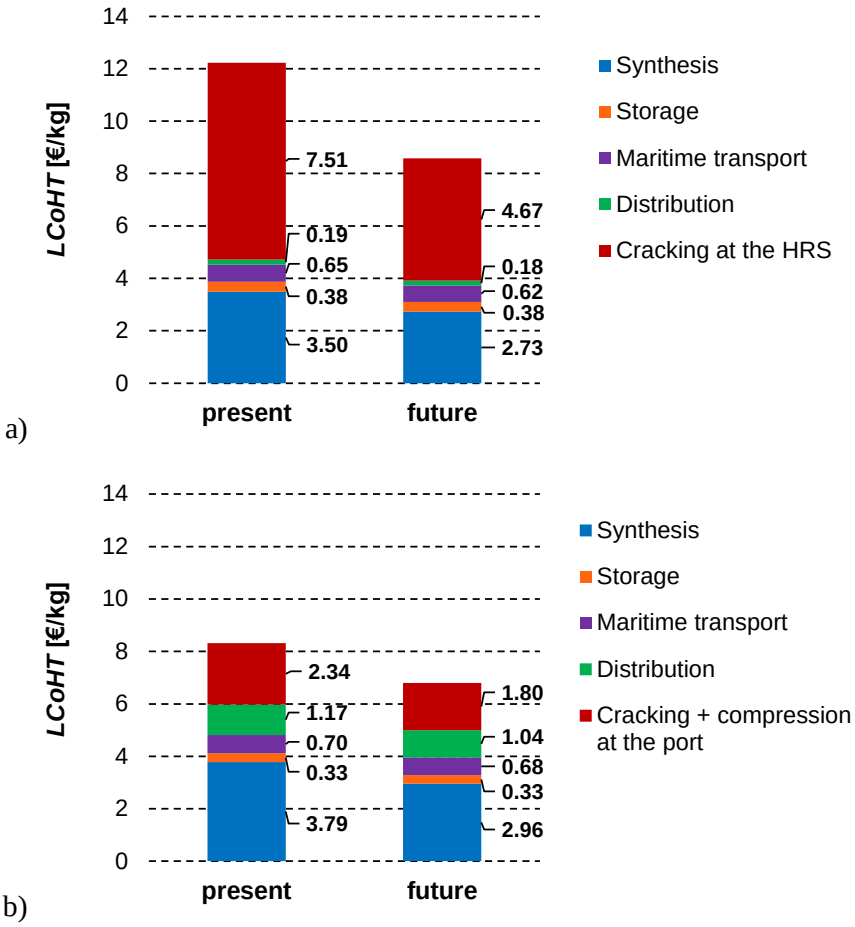

Fig. 8 – *LCoHT* [€/kg] in the case of hydrogen destination to HRS: comparison between the present and future scenarios when a) decentralized cracking occurs at the HRS and b) centralized cracking occurs at the port.

The overall *LCoHT* is 12.22 €/kg and 8.32 €/kg when considering, respectively, the decentralized or centralized ammonia reconversion to hydrogen in the "present" scenario. In the future, a reduction of these costs to 8.58 €/kg and 6.80 €/kg, respectively, is expected. In the case of hydrogen delivery to HRS, it is more cost-effective to carry out centralized cracking at the port of arrival and distributing compressed gaseous hydrogen than distributing liquefied ammonia and perform decentralized cracking at the refueling stations. In fact, referring to Fig. 8, the higher cost related to the compressed hydrogen road transport, in addition to the cost of

compression, is still lower than the cost of building and operating small-scale cracking plants at the HRS. However, a higher cost reduction is foreseen in the future for the decentralized cracking because at small-scale cracking reactors are run on electricity, instead of burning part of the ammonia delivered. Another aspect to consider is that, avoiding ammonia combustion, a greater hydrogen flow rate is delivered and, thus, more refueling stations can be served.

6. Conclusions

The techno-economic analysis carried out made it possible to deepen each single stage of the liquefied ammonia value chain for the transport of green hydrogen and to discuss the possible application in the industrial sector (H_2 valley) and in the mobility sector (Hydrogen Refueling Stations).

The application to the industrial sector is the one with the lowest costs since distribution to different end users is avoided. Among the investigated options for hydrogen delivery to HRS, currently the most cost-effective one involves centralized cracking at the port of arrival and distribution of compressed gaseous hydrogen. However, this option entails the safety issues associated with the management of gaseous hydrogen and a higher cost of distribution, since the number of trucks required is higher due to the lower hydrogen volumetric density. Moreover, the option involving decentralized cracking offers greater opportunities for reducing emissions: on the one hand, fewer trucks required for distribution result in a lower fuel consumption, on the other hand, the fact that small-scale cracking reactors are run on electricity involves the possibility of integration with renewable power.

In all the investigated cases, the cost drivers are the ammonia synthesis and cracking processes. Further research is advisable to reduce their costs: for the ammonia synthesis, the study of Haber-Bosch process intensification to reduce costs on a small-scale, for the ammonia cracking, the search for catalysts able to reduce the operating temperature.

References

[1] IRENA and AEA. Innovation Outlook: Renewable Ammonia. 2022.

[2] Valera-Medina A, Xiao H, Owen-Jones M, David WIF, Bowen PJ. Ammonia for power. Progress in Energy and combustion science. 2018;69:63-102.

[3] https://www.portofrotterdam.com/en/news-and-press-releases/development-of-import-terminal-for-hydrogen-carrier-in-port-of-rotterdam. [Accessed 24 March 2023].

[4] https://www.ammoniaenergy.org/articles/saudi-arabia-to-export-renewable-energy-using-green-ammonia/. [Accessed 24 March 2023].

[5] Sadler D, Anderson HS, Sperrink M, Cargill A, Sjovoll M, Asen K, et al. H21 North of England. 2018. Report, Northern Gas Networks, Leeds. 2018.

[6] Okunlola A, Giwa T, Di Lullo G, Davis M, Gemechu E, Kumar A. Techno-economic assessment of low-carbon hydrogen export from Western Canada to Eastern Canada, the USA, the Asia-Pacific, and Europe. International Journal of Hydrogen Energy. 2022;47:6453-77.

[7] Berger R. Hydrogen transportation. 2021.

[8] Song S, Lin H, Sherman P, Yang X, Nielsen CP, Chen X, et al. Production of hydrogen from offshore wind in China and cost-competitive supply to Japan. Nature communications. 2021;12:6953.

[9] Gallardo FI, Ferrario AM, Lamagna M, Bocci E, Garcia DA, Baeza-Jeria TE. A Techno-Economic Analysis of solar hydrogen production by electrolysis in the north of Chile and the case of exportation from Atacama Desert to Japan. international journal of hydrogen energy. 2021;46:13709-28.
[10] Hong X, Thaore VB, Karimi IA, Farooq S, Wang X, Usadi AK, et al. Techno-enviro-economic analyses of hydrogen supply chains with an ASEAN case study. International Journal of Hydrogen Energy. 2021;46:32914-28.
[11] Chodorowska N, Farhadi, M. H2 value chain comparing different transport vectors. GPA Europe Virtual Conference, 25 May 2021.
[12] Papadias DD, Peng J-K, Ahluwalia RK. Hydrogen carriers: Production, transmission, decomposition, and storage. International Journal of Hydrogen Energy. 2021;46:24169-89.
[13] Hydrogen Import Coalition. Shipping sun and wind to Belgium is key in climate neutral economy. Technology. 2021;14:19.
[14] Wijayanta AT, Oda T, Purnomo CW, Kashiwagi T, Aziz M. Liquid hydrogen, methylcyclohexane, and ammonia as potential hydrogen storage: Comparison review. International Journal of Hydrogen Energy. 2019;44:15026-44.
[15] Hank C, Sternberg A, Köppel N, Holst M, Smolinka T, Schaadt A, et al. Energy efficiency and economic assessment of imported energy carriers based on renewable electricity. Sustainable Energy & Fuels. 2020;4:2256-73.
[16] Ishimoto Y, Voldsund M, Nekså P, Roussanaly S, Berstad D, Gardarsdottir SO. Large-scale production and transport of hydrogen from Norway to Europe and Japan: Value chain analysis and comparison of liquid hydrogen and ammonia as energy carriers. International Journal of Hydrogen Energy. 2020;45:32865-83.
[17] IEA. The Future of Hydrogen. 2019.
[18] https://www.cliffordchance.com/content/dam/cliffordchance/briefings/2022/08/focus-on-hydrogen-in-japan.pdf. [Accessed 24 March 2023].
[19] AspenTech. Aspen Plus®, Burlington (MA), United States. 2019.
[20] Martin J, Neumann A, Ødegård A. Sustainable Hydrogen Fuels Versus Fossil Fuels for Trucking, Shipping and Aviation: A Dynamic Cost Model: MIT Center for Energy and Environmental Policy Research; 2022.
[21] Lorenczik S, Kim S, Wanner B, Bermudez Menendez JM, Remme U, Hasegawa T, et al. Projected costs of generating electricity-2020 edition. 2020.
[22] https://www.ecb.europa.eu/stats/policy_and_exchange_rates/euro_reference_exchange_rates/html/eurofxref-graph-usd.en.html. [Accessed 24 March 2023].
[23] Turton R, Bailie RC, Whiting WB, Shaeiwitz JA. Analysis, synthesis and design of chemical processes: Pearson Education; 2008.
[24] Guthrie KM. Capital Cost Estimating. Chemical Engineering. 1969;76:114.
[25] Cesaro Z, Ives M, Nayak-Luke R, Mason M, Bañares-Alcántara R. Ammonia to power: Forecasting the levelized cost of electricity from green ammonia in large-scale power plants. Applied Energy. 2021;282:116009.
[26] Private communication with Thermal Dynamix™. 8 November 2022.
[27] Makhloufi C, Kezibri N. Large-scale decomposition of green ammonia for pure hydrogen production. International Journal of Hydrogen Energy. 2021;46:34777-87.
[28] Spatolisano E, Matichecchia A, Pellegrini LA, De Angelis AR, Cattaneo S, Roccaro E. Toluene as effective LOHC: detailed techno-economic assessment to identify challenges and opportunities. 33rd European Symposium on Computer-Aided Process Engineering (ESCAPE), 18-21 June 2023.
[29] https://worldsalaries.com/. [Accessed 31 May 2023].
[30] Rogers H. LNG Shipping Forecast: costs rebounding, outlook uncertain. 2018.
[31] https://www.shipfinance.dk/media/2054/shipping-market-review-november-2020.pdf. [Accessed 24 March 2023].
[32] https://capitallinkshipping.com/wp-content/uploads/2022/10/Intermodal-Report-Week-41-2022_compressed.pdf. [Accessed 24 March 2023].
[33] https://www.mis.gr/docs/gdestiny/gdestiny-2022-11.pdf. [Accessed 24 March 2023].

[34] https://www.hellenicshippingnews.com/wp-content/uploads/2021/10/Weekly-SP-Market-Report-Week-ending-October-29th-2021-Week-43-Report-No-43.21.pdf. [Accessed 24 March 2023].
[35] https://www.hartmann-reederei.de/shared_files/fleet/pdf/ship-info/phoenix.pdf. [Accessed 24 March 2023].
[36] https://www.eia.gov/environment/emissions/co2_vol_mass.php. [Accessed 24 March 2023].
[37] Bartels JR. A feasibility study of implementing an Ammonia Economy: Iowa State University; 2008.
[38] https://arpa-e.energy.gov/sites/default/files/03%20ARPA-E%20REFUEL%20Kickoff%20Meeting%20%20%208-16-17.pdf. [Accessed 24 March 2023].
[39] Leighty WC, Holbrook JH. Alternatives to electricity for transmission and low-cost firming storage of large-scale stranded renewable energy as pipelined hydrogen and ammonia carbon-free fuels.
[40] Graf M. Costs and energy efficiency of long-distance hydrogen transport options [Master Thesis]. Vienna: University of Natural Resources and Life Sciences; 2021.
[41] Reuß M, Grube T, Robinius M, Preuster P, Wasserscheid P, Stolten D. Seasonal storage and alternative carriers: A flexible hydrogen supply chain model. Applied energy. 2017;200:290-302.
[42] Agrawal R, Thorogood RM. Production of medium pressure nitrogen by cryogenic air separation. Gas separation & purification. 1991;5:203-9.
[43] Mok L. Sensitivity study of energy consumption in ammonia plant operation. 1982.
[44] Nielsen A, Kjaer J, Hansen B. Rate equation and mechanism of ammonia synthesis at industrial conditions. Journal of Catalysis. 1964;3:68-79.
[45] Lucentini I, Garcia X, Vendrell X, Llorca J. Review of the decomposition of ammonia to generate hydrogen. Industrial & Engineering Chemistry Research. 2021;60:18560-611.
[46] Spatolisano E, Pellegrini LA, De Angelis AR, Cattaneo S, Roccaro E. Ammonia as a carbon-free energy carrier: NH3 cracking to H2. Submitted to Industrial & Engineering Chemistry Research. 2023.
[47] Morgan ER. Techno-economic feasibility study of ammonia plants powered by offshore wind: University of Massachusetts Amherst; 2013.